

Highly sensitive ppb-level H₂S gas sensor based on fluorophenoxy-substituted phthalocyanine cobalt/rGO hybrids at room temperature

Bin Wang,^{*a} Xiaolin Wang,^b ZhiJiang Guo,^a Shijie Gai,^a Yiqun Wu,^{ac}

^aKey Laboratory of Functional Inorganic Material Chemistry, Ministry of Education,
School of Chemistry and Materials Science, Heilongjiang University, Harbin 150080, P.
R. China. E-mail: wangbin@hlju.edu.cn.

^bSchool of Material and Chemical Engineering, Heilongjiang Institute of Technology,
Harbin 150050, P. R. China

^cShanghai Institute of Optics and Fine Mechanics, Chinese Academy of Sciences,
Shanghai 201800, P. R. China.

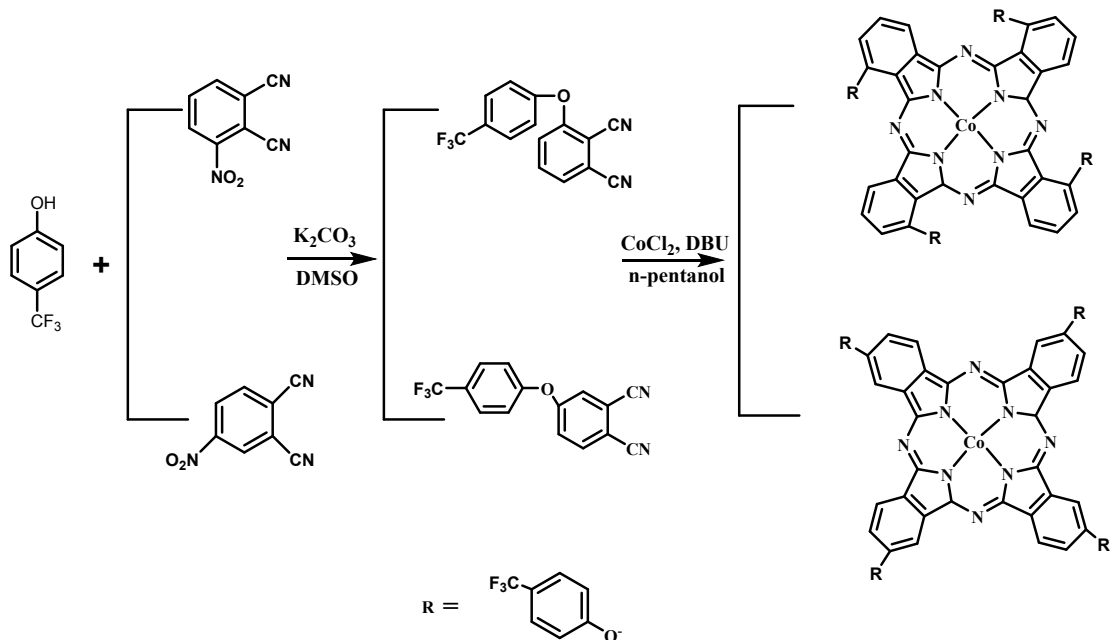
Tel.: +86 451 86609121

Fax: +86 451 86673647

1. Experimental detail

1.1 Materials

All chemicals were analytical grade and commercially available and used without further purification. 3-nitrophthalonitrile and 4-nitrophthalonitrile was purchased from Sigma-Aldrich Co. LLC., and was used without further purification. The synthesis scheme of Tetra- α -trifluoromethylphenoxyphthalocyanine cobalt (3-cF₃poPcCo), and Tetra- β -trifluoromethylphenoxyphthalocyanine cobalt (4-cF₃poPcCo) is shown in scheme S1.



Scheme S1. Synthesis scheme of 3-cF₃poPcCo and 4-cF₃poPcCo.

1.2 The structure for gas sensors

Al₂O₃ ceramic substrate is used for gas sensors. TaN, TiW, Ni and Au are sputtered on substrate as resistive layer, supporting layer, solder mask and conductor layer, respectively. Standard photolithography is then used to create Au interdigitated electrodes with 180 μ m electrode widths, and 50 μ m electrode gaps.

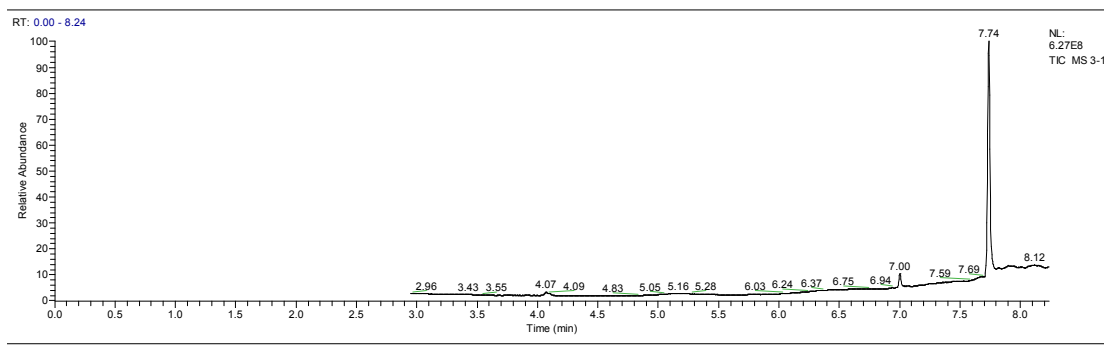
1.3 Characterization

Scanning electron microscopy (SEM) images were recorded with a Hitachi S-4800 field emission scanning electron microscope operating at 15 kV. Samples were drop-deposited onto the interdigitated electrodes and measured directly. UV/Vis absorption

spectra were recorded with an UV-2700 spectrometer (SHIMADZU, Japan). FT-IR spectra were recorded on a Spectrum two spectrometer (Perkin-Elmer).

1.4 Synthesis of 3 - (4-trifluoromethylphenoxy) phthalonitrile

3-Nitrophthalonitrile (1.06 g, 5.78 mmol) was dissolved in DMSO (10 mL) under a nitrogen atmosphere, and then P-trifluoromethylphenol (1.41 g, 8.7 mmol) was added to the solution. After stirring for 1h, the mixture of anhydrous potassium carbonate (K_2CO_3) (3g, 21.7mmol) was added one by one and stirred for 3 days in nitrogen atmosphere at room temperature. After the reaction, cool the reaction mixture to room temperature and pour it into about 200ml of ice water medium. After standing for about 24 hours, the white emulsion precipitates will be separated, and then the precipitates will be washed with a large amount of deionized water until the washing solution becomes neutral. Then the mixture of $CHCl_3$: MeOH (100/2) was used to separate pure white crystal products on silica gel column. The molecular weight of 3 - (4-trifluoromethylphenoxy) phthalonitrile analyzed by gas chromatography-mass spectrometry is shown in Fig. S1. Similarly, after the conversion of 3-phthalonitrile to 4-phthalonitrile. The same method can also be used to prepare 4 - (4-trifluoromethylphenoxy) phthalonitrile. The molecular weight of 4 - (4-trifluoromethylphenoxy) phthalonitrile analyzed by gas chromatography-mass spectrometry is shown in Fig. S2.



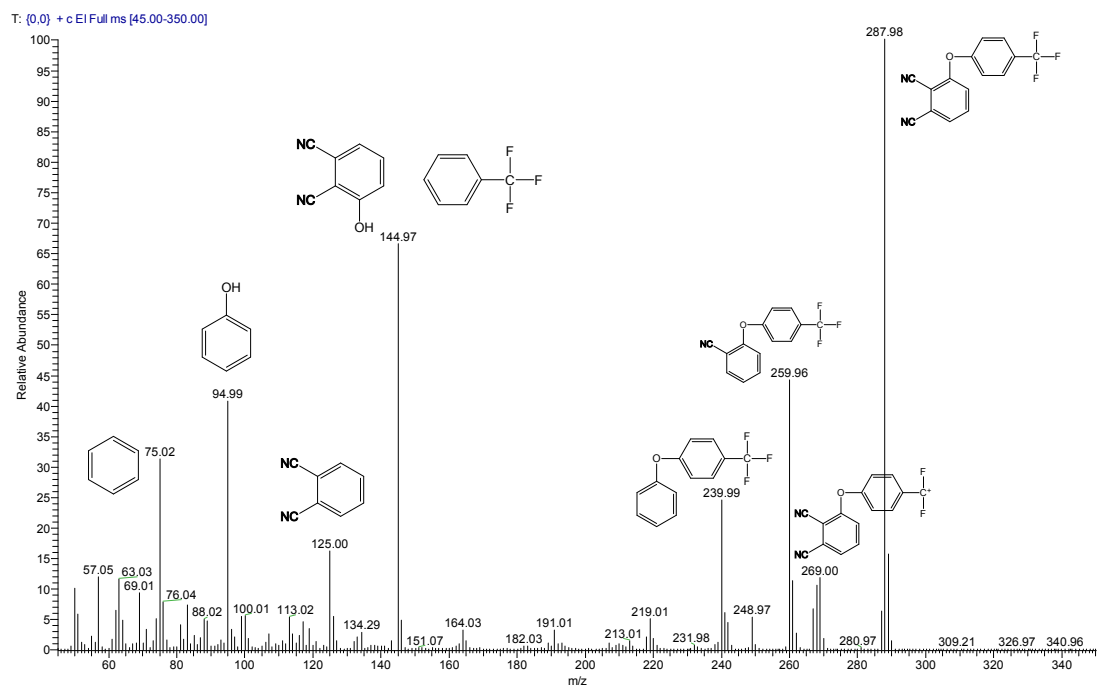
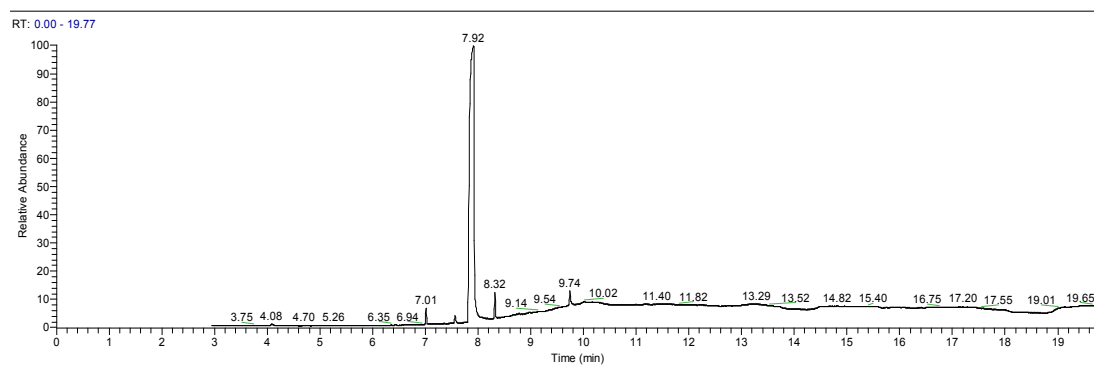


Fig.S1 GC-MS of 3-(4-trifluoromethylphenoxy) phthalonitrile.



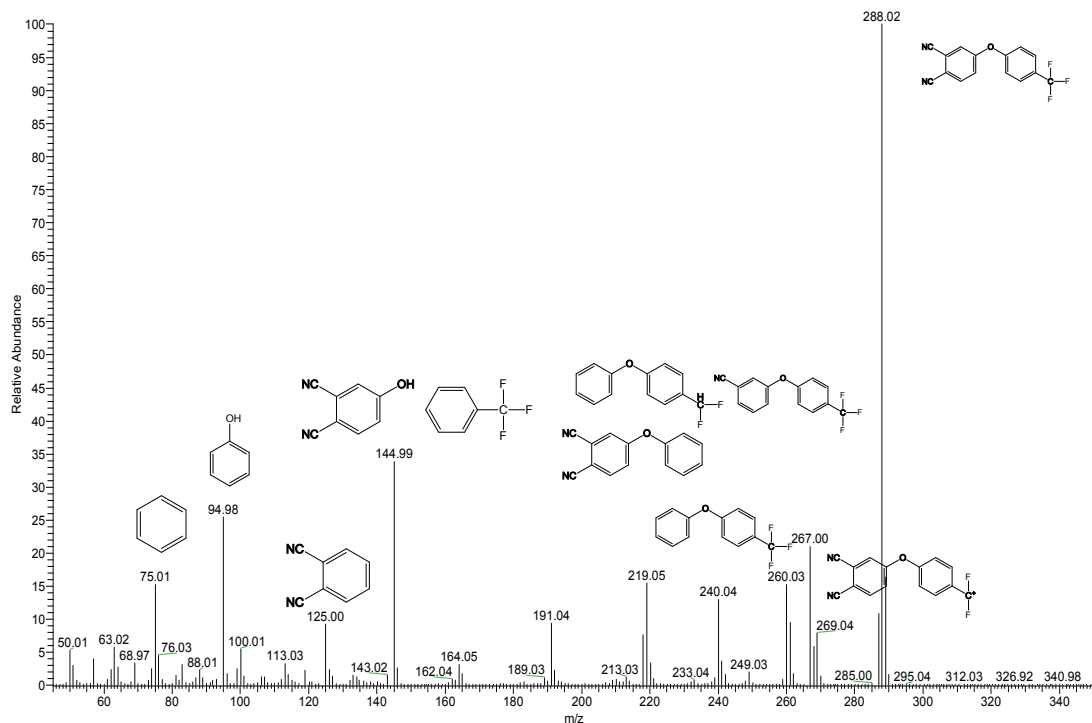


Fig.S2 GC-MS of 4-(4-trifluoromethylphenoxy)phthalonitrile

1.5 Synthesis of trifluoromethylphenoxyphthalocyanine cobalt

At room temperature, 3-(4-trifluoromethylphenoxy) phthalonitrile (1.06 g, 3.69 mmol), anhydrous cobalt chloride (II) (0.16 g, 1.23 mmol) and DBU (2.0 mL) were added to distilled n-pentanol (30 mL). The subsequent mixture was continuously stirred under reflux for 10 hours under a nitrogen atmosphere. After naturally cooling to about 20 °C, the precipitate was filtered, washed sequentially with methanol (50 mL) and acetone (50 mL). The pure crystal product 3-cF₃poPcCo was obtained by chromatographic separation on silica gel column with acetone and dichloromethane (4:1) mixed solvent. Finally, the purple black crystal was obtained by drying in a vacuum oven at 50 °C. Similarly, after 3 - (4-trifluoromethylphenoxy) phthalonitrile is converted to 4 - (4-trifluoromethylphenoxy) phthalonitrile. The same method can also be used to prepare 4-cF₃poPcCo.

2. Result and discussion

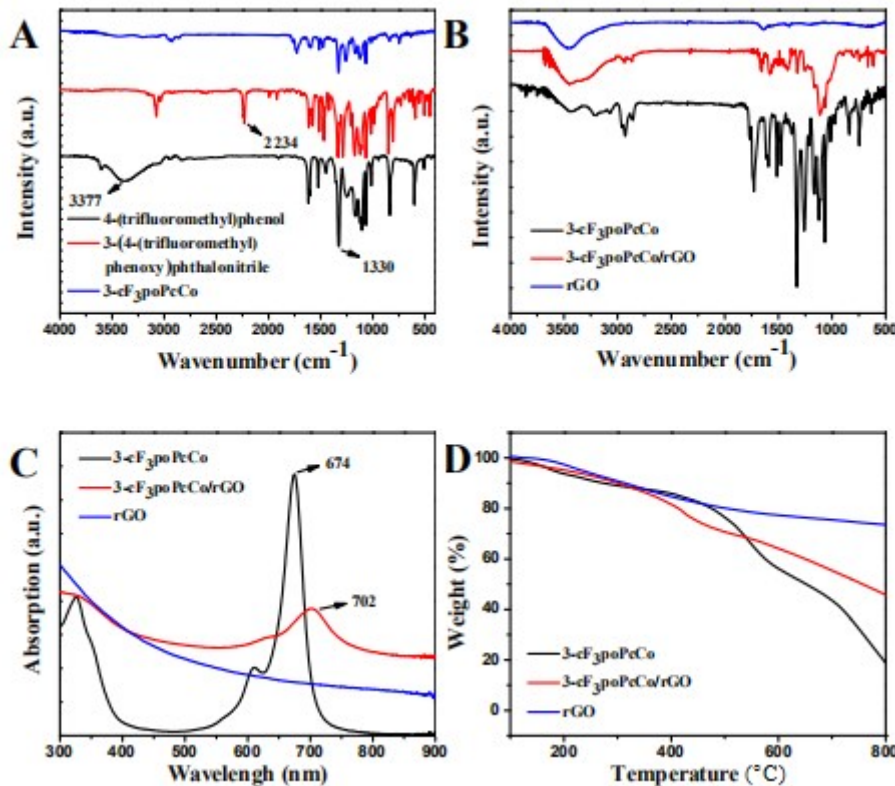


Fig.S3 (A) FT-IR spectra of 4-(trifluoromethyl) phenol, 3 - (4-trifluoromethylphenoxy) phthalonitrile and 3-cF₃poPcCo hybrids; (B) FT-IR spectra of rGO, 3-cF₃poPcCo and 3-cF₃poPcCo/rGO hybrids; (C) UV-vis spectra of rGO, 3-cF₃poPcCo and 3-cF₃poPcCo/rGO hybrids in DMF; (D) TG profiles of rGO, 3-cF₃poPcCo and 3-cF₃poPcCo/rGO hybrid.

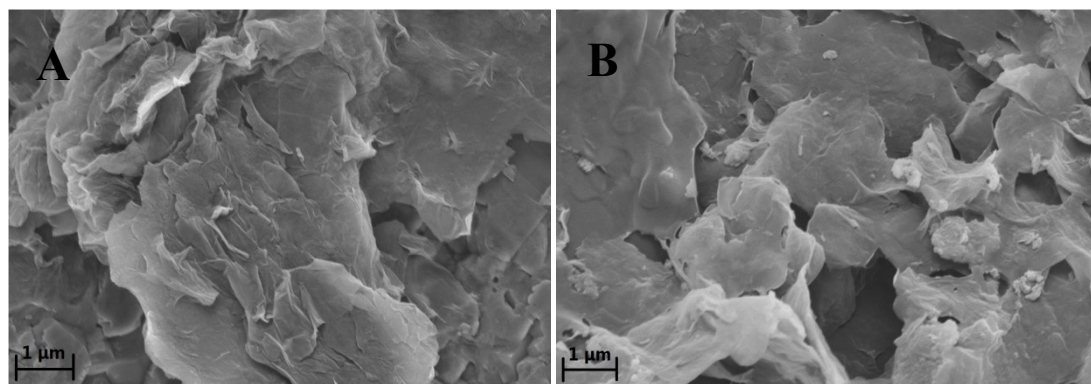


Fig.S4 The microstructure of (A) 3-cF₃poPcCo/rGO and (B) 4-cF₃poPcCo/rGO hybrid.

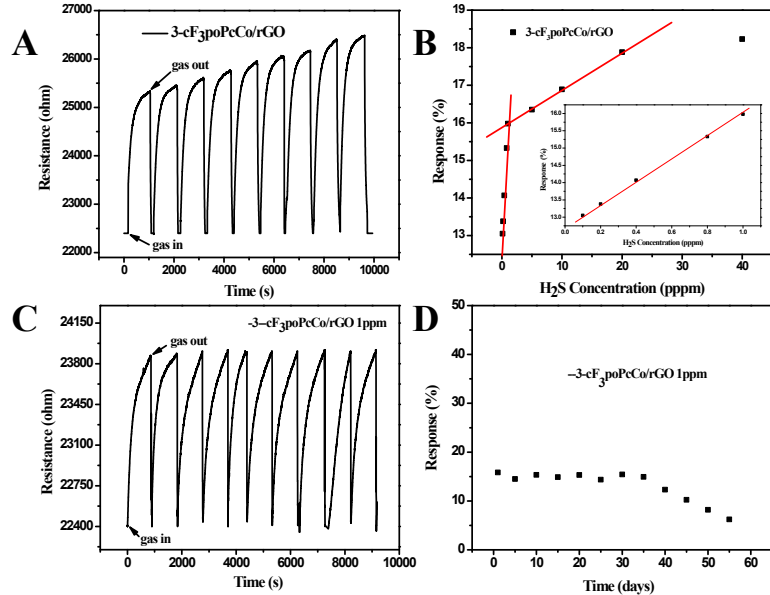


Fig.S5 (A) Resistance of the $3\text{-cF}_3\text{poPcCo/rGO}$ hybrid sensor upon exposure to varying concentrations of H_2S ; (B) relationship of the response of the $3\text{-cF}_3\text{poPcCo/rGO}$ hybrid sensor to the concentration H_2S ; (C) ten sensing cycles of the $3\text{-cF}_3\text{poPcCo/rGO}$ hybrid sensor to 1 ppm H_2S ; (D) the reproducibility characteristics of the $3\text{-cF}_3\text{poPcCo/rGO}$ hybrid sensor to 1 ppm H_2S within 60 days at 25 °C.

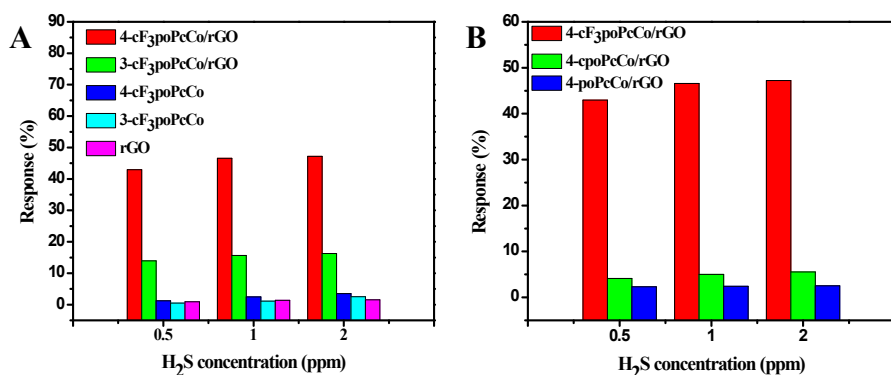


Fig.S6 (A) Response of 4-cF₃poPcCo/rGO, 3-cF₃poPcCo/rGO, 4-cF₃poPcCo, 3-cF₃poPcCo and

rGO sensors upon varying the concentration of H₂S; (B) Response of 4-cF₃poPcCo/rGO, 4-cpoPcCo, 4-poPcCo sensors upon varying the concentration of H₂S.

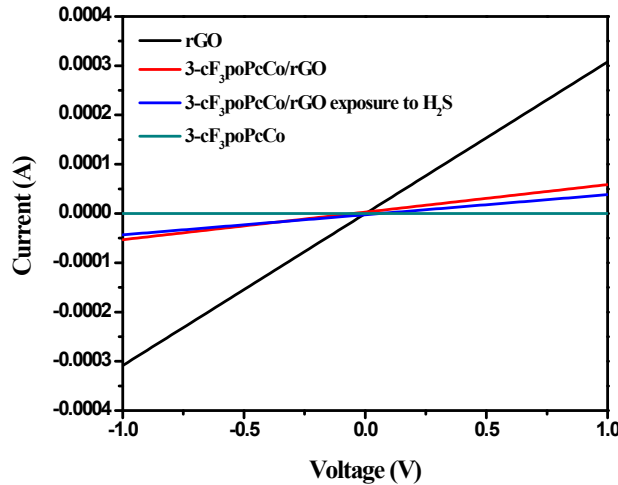


Fig.S7 I-V curves of the rGO, 3-cF₃poPcCo, 3-cF₃poPcCo/rGO and 3-cF₃poPcCo/rGO exposure to H₂S.

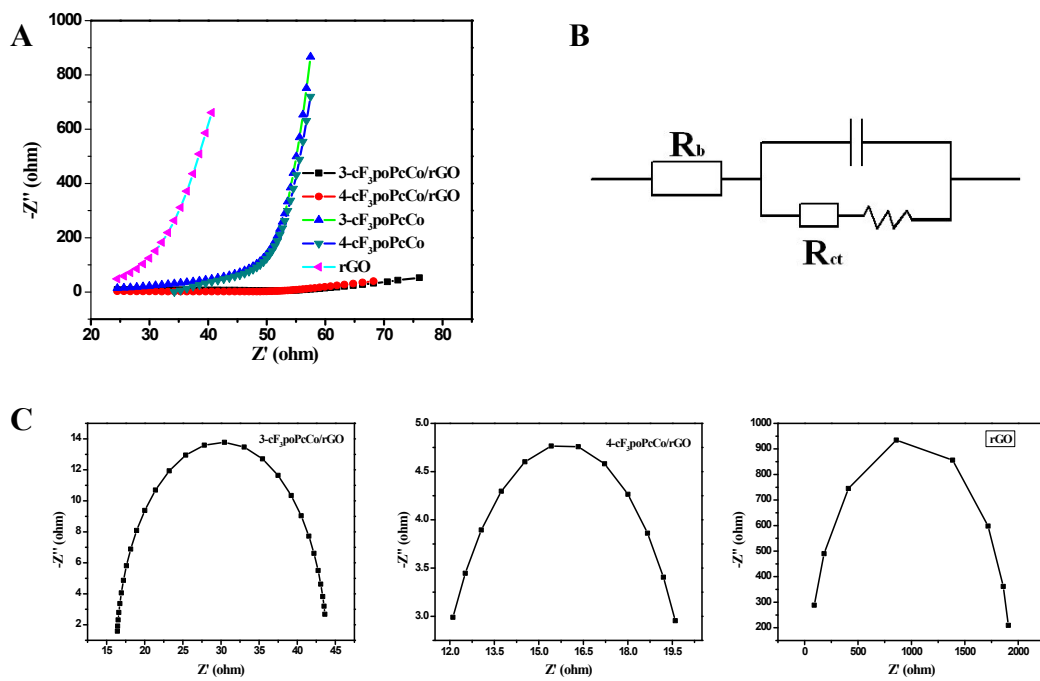


Fig.S8 (A) Nyquist plots of rGO, cF₃poPcCo, cF₃poPcCo/rGO hybrids and (B) Equivalent circuit diagram; (C) Fitted chemical impedance Nyquist plots of rGO and cF₃poPcCo/rGO hybrids.

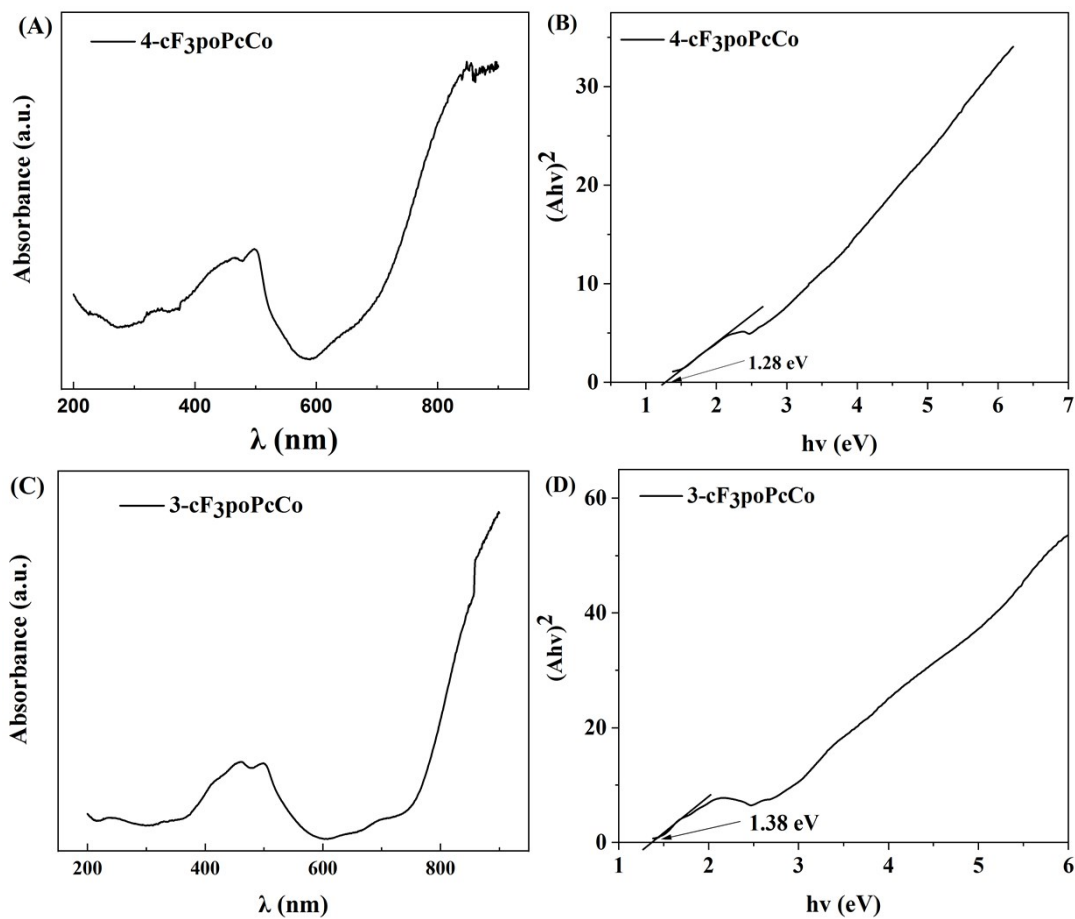


Fig. S8. UV-vis absorption spectra (A,C) and band gap energies (B,D) of 4-cF₃poPcCo and 3-cF₃poPcCo.

Table S1. Comparison of the detection performances of different H₂S sensors

Sensor material	Response(%)/Detection conc. (ppm) ^[b]	Detection limit(ppm) ^[a]	Working temperature (°C) ^[c]	Recovery time (s)/Detection conc.(ppm) ^[b]	Detection range (ppm)	Ref.
net-like SnO ₂ /ZnO	112/5	0.01	100	513/5	0.5-10	1
In ₂ O ₃	1.4/10	0.2	RT	~7200/100	10-80	2
CuO-Decorated ZnO	83.5/5	0.015	200	65/5	5-100	3
Cu/SWCNTs	1.3/20	—	RT	20/20	5-150	4

PPy/WO ₃	5.3/1	—	RT	12600/1	0.1-1	5
Co phthalocyanine-Au	5.2/10	0.1	RT	960/10	0.1-50	6
SnO ₂ multtube arrays	1.5/5	—	RT	30/5	5-100	7
SnO ₂ -CNT	4/50	~9	RT	~60/50	~50-~200	8
quasi-2D CuO/SnO ₂	1.8/50	0.5	RT	500/50	0.5-100	9
Cu ₂ O-FGS	1.4/0.1	0.005	RT	—	0.005-0.1	10
SnO ₂ nanowire/rGO	33/50	0.043	RT	292/50	10-100	11
Au/Fe ₂ O ₃	6.38/10	1	250	1620/10	1-50	12
p-type Co ₃ O ₄	4.5/100	0.3	300	24/100	1-100	13
SnO ₂ -rGO	34.31/100	0.042	125	900/100	1-100	14
CuO	1.25/0.01	—	RT	76/0.01	0.01-60	15
TiO ₂ /α-Fe ₂ O ₃	7.4/200	—	300	180/200	1-200	16
AlGaN/GaN	112/90	—	250	507/90	15-90	17
α-Fe ₂ O ₃	5.8/5	—	135	45/5	1-50	18
SnO ₂ -CuWO ₄	2 × 10 ⁶ (sensor signal)/20	—	100	438/20	5-30	19
SnO ₂ -CuO	38/100	—	100	Long/120	0.1-30	20
cF ₃ poPcCo/rGO	15.63/1	0.023	RT	120/1	0.1-40	This work ^[d]
cF ₃ poPcCo/rGO	46.58/1	0.0116	RT	50/1	0.1-40	

[a] If the sensor detection limit was not explicitly provided in the original report, then the lowest tested analyte concentration is listed.

[b] If the response (%), response time (s) or recovery time (s) of the sensor was not explicitly provided in the original report, then the estimate from the curve in that report is listed.

[c] RT, abbreviation for room temperature.

[d] sensor prepared with the cF₃poPcCo/rGO aqueous dispersion concentrations of 1.0 mg ml⁻¹.

- [1]D. Y. Fu, C. L. Zhu, X. T. Zhang, C. Y. Li, Y. J. Chen, Two dimensional net-like SnO₂/ZnO heteronanostructures for highperformance H₂S gas sensor. *J. Mater. Chem. A* 2016, 4, 1390.
- [2]M. Kaur, N. Jain, K. Sharma, S. Bhattacharya, M. Roy, A.K. Tyagi, S.K. Gupta, J.V. Yakhmi, Room-temperature H₂S gas sensing at ppb level by single crystal In₂O₃ whiskers. *Sens. Actuators, B* 2008, 133, 456–461.
- [3]N.M. Vuong, N.D. Chinh, B.T Huy, Y. Lee CuO-Decorated ZnO Hierarchical Nanostructures as Efficient and Established Sensing Materials for H₂S Gas Sensors, *Sci.Rep.* 6:26736.
- [4]M. Asad, M.H. Sheikhi, M. Pourfath, M. Moradi, High sensitive and selective flexible H₂S gas sensors based on Cu nanoparticle decorated SWCNTs, *Sens. Actuators, B* 2015, 210, 1–8.
- [5]P.G.Su, Y.T. Peng, Fabrication of a room-temperature H₂S gas sensor based on PPy/WO₃ nanocomposite films by in-situ photopolymerization, *Sens. Actuators, B* 2014, 193, 637–643.
- [6]A. Kumar, N. Joshi, S. Samanta, A. Singh, A.K. Debnath, A.K. Chauhan, M. Roy, R. Prasad, K. Roy, M.M. Chehimi, D.K. Aswal, S.K. Gupta, Room temperature detection of H₂S by flexible gold–cobalt phthalocyanine heterojunction thin films, *Sens. Actuators,B* 2015, 206, 653–662.
- [7]J. Tian, F. Pan, R. Xue, W. Zhang, X. Fang, Q. Liu, Y. Wang, Z. Zhang, D. Zhang, A highly sensitive room temperature H₂S gas sensor based on SnO₂ multi-tube arrays bio-templated from insect bristles, *Dalton Trans.* 2015, 44, 7911–7916.
- [8]F. Mendoza, D.M. Hernández, V. Makarov, E. Febus, B.R. Weiner, G. Morell, Room temperature gas sensor based on tin dioxide–carbon nanotubes composite films. *Sens. Actuators, B* 2014, 190, 227–233.
- [9]G. Cui, M. Zhang, G. Zou, Resonant tunneling modulation in quasi-2D Cu₂O/SnO₂ p–n horizontal-multi-layer heterostructure for room temperature H₂S sensor application. *Sci.Rep.* 2013, 3, 1250.
- [10]L. Zhou, F. Shen, X. Tian, D. Wang, T. Zhang, W. Chen, Stable Cu₂O nanocrystals grown on functionalized graphene sheets and room temperature H₂S gas sensing with ultrahigh sensitivity, *Nanoscale* 2013, 5, 1564–1569.
- [11]Z.L. Song, Z.R. Wei, B.C. Wang, Z. Luo, S.M. Xu, W.K. Zhang, H.X. Yu, M. Li, Z. Huang, J.F. Zang, F. Yi, H. Liu, Sensitive Room-Temperature H₂S Gas Sensors Employing SnO₂ Quantum Wire/Reduced Graphene Oxide Nanocomposites, *Chem. Mater.* 2016, 28, 1205–1212.

- [12]V. Balouria, N.S. Ramgir, A. Singh, A.K. Debnath, A. Mahajan, R.K. Bedi, D.K. Aswal, S.K. Gupta, Enhanced H₂S sensing characteristics of Au modified Fe₂O₃ thin films, *Sens. Actuators B* 2015, 219, 125–132.
- [13]P.L. Quang, N.D. Cuong, T.T. Hoa, H.T. Long, C.M. Hung, D.T.T. Le, N.V. Hieu, Simple post-synthesis of mesoporous p-type Co₃O₄ nanochains for enhanced H₂S gas sensing performance, *Sens. Actuators B* 2018, 270, 158–166.
- [14]J. Chu, X. Wang, D. Wang, A. Yang, P. Lv, Y. Wu, M. Rong, L. Gao, Highly selective detection of sulfur hexafluoride decomposition components H₂S and SOF₂ employing sensors based on tin oxide modified reduced graphene oxide *Carbon* 2018, 135, 95–103.
- [15]Z. Li, N. Wang, Z. Lin, J. Wang, W. Liu, K. Sun, Y.Q. Fu, Z. Wang, Room-Temperature High-Performance H₂S Sensor Based on Porous CuO Nanosheets Prepared by Hydrothermal Method, *ACS Appl. Mater. Interfaces* 2016, 8, 20962–20968.
- [16]H. Kheel, G.J. Sun, J.K. Lee, S. Lee, R.P. Dwivedi, C. Lee, Enhanced H₂S sensing performance of TiO₂-decorated α -Fe₂O₃ nanorod sensors, *Ceram. Int.* 2016, 42, 18597–18604.
- [17]R. Sokolovskij, J. Zhangb, E. Iervolino, C. Zhao, F. Santagata, F. Wang, H. Yu, P.M. Sarro, G.Q. Zhang, Hydrogen sulfide detection properties of Pt-gated AlGaN/GaN HEMT-sensor, *Sens. Actuators B* 2018, 274, 636–644.
- [18]D. Li, L. Qin, P. Zhao, Y. Zhang, D. Liu, F. Liu, B. Kang, Y. Wang, W.H. Song, T. Zhang, G.Y. Lu, Preparation and gas-sensing performances of ZnO/CuO rough nanotubular arrays for low-working temperature H₂S detection. *Sens. Actuators B* 2018, 254, 834–841.
- [19]A. Stanoiu, C.E. Simion, J.M. Calderon-Moreno, P. Osiceanu, M. Florea, V.S. Teodorescu, S. Somacescu, Sensors based on mesoporous SnO₂-CuWO₄ with high selective sensitivity to H₂S at low operating temperature, *J. Hazard. Mater.* 2017, 331, 150–160.
- [20]C. Gao, Z.D. Lin, N. Li, P. Fu, X.H. Wang, Preparation and H₂S Gas-Sensing Performances of Coral Like SnO₂-CuO Nanocomposite, *Acta Metall. Sin. (Engl. Lett.)* 2015, 28, 1190–1197.

